Hot versus Cold Hidden Sectors and Their Effects on Thermal Relics

Jinzheng Li and Pran Nath

Northeastern University, Boston, Massachusetts 02115-5005, USA

Abstract

A variety of possibilities exist for dark matter aside from WIMPS, such as hidden sector dark matter. We discuss the synchronous thermal evolution of visible and hidden sectors and show that the density of thermal relics can change O(100%) and $\Delta N_{\rm eff}$ by a factor of up to 10^5 depending on whether the hidden sector was hot or cold at the reheat temperature. It is also shown that the approximation of using separate entropy conservation for the visible and hidden sectors is invalid even for a very feeble coupling between the two.

Keywords: Hidden sectors, dark matter, thermal evolution *DOI*: 10.31526/LHEP.2024.502

1. INTRODUCTION

In exploration of Physics Beyond the Standard Model, hidden sectors play a role in a variety of settings such as in supergravity (for a review see [1]), in strings [2], in branes [3], and in moose/quiver theories [4]. Much like the visible sector the hidden sector could contain gauge fields and matter fields, and it is altogether possible that dark matter may reside in the hidden sector. The success of the electroweak physics in the standard model indicates that the coupling of the hidden sector with the visible sector must be feeble. On the other hand, the coupling of the hidden sector with the inflaton is largely unknown. Thus, the couplings of the hidden sector with the inflaton could be as strong as those of the standard model leading to the hidden sector being hot with $\xi(T) \equiv \frac{T_h}{T}|_{RH} \simeq 1$, where $T(T_h)$ is the visible (hidden) sector temperature and RH refers to the reheat temperature of the universe. Alternately, the hidden sector may not couple or may have suppressed couplings with the inflaton in which case $\xi_0 \simeq 0|_{RH}$. It is then of interest to determine the evolution of $\xi(T) = T_h/T$ as a function of T. This is of importance since $\xi(T)$ enters the analysis of observable physics such as the relic density, dark matter cross sections, $\Delta N_{\rm eff}$ at BBN, and other low energy observables. Recently, the evolution equation for $\xi(T)$ has been derived from energy conservation [5, 6, 7], i.e.,

$$\frac{d\rho_v}{dt} + 3H(\rho_v + p_v) = j_v \text{ (visible sector)},\tag{1}$$

$$\frac{d\rho_h}{dt} + 3H\left(\rho_h + p_h\right) = j_h \text{ (hidden sector)},\tag{2}$$

where $\rho_v(\rho_h)$ is the energy density of the visible (hidden) sector, $p_v(p_h)$ is the pressure for the visible (hidden sector), (j_v, j_h) are the sources, and H is the Hubble parameter. A straightforward analysis leads to the following differential equation for $\xi(T)$:

$$\frac{d\xi}{dT} = \left[-\xi \frac{d\rho_h}{dT_h} + \frac{4H\eta_h\rho_h - j_h}{4H\eta_\rho - 4H\eta_h\rho_h + j_h} \frac{d\rho_v}{dT} \right] \left(T \frac{d\rho_h}{dT_h} \right)^{-1}, \quad (3)$$

where $\eta=1$ (radiation dominance), and $\eta=3/4$ (matter dominance). We note in passing that the assumption of separate entropy conservation of the visible and the hidden sectors to estimate $\xi(T)$ (see, e.g., [8, 9]) could deviate substantially from the true value even for very feeble coupling between the sectors as discussed in Section 3.4.

2. A HIDDEN SECTOR MODEL

As a concrete example of a hidden sector, we consider a $U(1)_X$ extension of the standard model with a particle content consisting of a gauge boson (C_u), a Dirac fermion (D) charged under $U(1)_X$ with a gauge coupling constant g_X , and spin zero dark fields ϕ , s. Communication with the visible sector occurs via kinetic mixing [10] or Stueckelberg mass mixing [11] between the $U(1)_X$ gauge field C_μ and the hypercharge $U(1)_Y$ gauge field B_{μ} of the standard model. The communication between the two can also take place via a combined kinetic-Stueckelbergmass mixing [12], via a Stueckelberg-Higgs mixing [13], and via a variety of other mechanisms such as via Higgs portal [14] and higher dimensional operators. In the case of kinetic mixing, one adds a gauge invariant combination $\frac{\delta}{2}C^{\mu\nu}B_{\mu\nu}$, and for the Stueckelberg mass mixing, one adds $(m_1C_\mu + m_2B_\mu + \partial_\mu\sigma)^2$ where σ is an axionic field which transforms dually under $U(1)_X$ and $U(1)_Y$ to keep the mass mixing term gauge invariant. In the mass and kinetic energy diagonal basis for the gauge bosons, one will have a massive dark photon γ' with mass $m_{\gamma'}$ in addition to the standard model gauge bosons W^{\pm} , Z. The mass mixing mechanism generates a milli-charge on the hidden sector matter [11, 15], and such matter is relevant in the explanation of EDGES anomaly [16]. This letter is a brief discussion of the main results of the consequences of hidden sector initial conditions at the reheat temperature on thermal relics and a more detailed version of the analysis will appear in [17]. In the following, we discuss some of the observable consequences of a hot vs a cold hidden sector at the reheat time.

3. THERMAL EFFECTS ON OBSERVABLES

3.1. Dark Matter Relics

As the preceding discussion indicates, the visible and the hidden sectors will in general be in different heat baths. In the presence of couplings between the two sectors even feeble, a consistent analysis requires that one carry out a synchronous thermal evolution of the two sectors. Such a synchronous evolution requires solution to $\xi(T)$ given by equation (3). A solution to $\xi(T)$ also requires a simultaneous solution to the yield equations for the dark fermion D and the dark photon γ' which results from the $U(1)_X$ gauge field acquiring mass. We exhibit below the

yield equations

$$\frac{dY_{D}}{dT} = F(T) \left[\langle \sigma v \rangle_{D\bar{D} \to i\bar{i}} (T) Y_{D}^{eq} (T)^{2} - \langle \sigma v \rangle_{D\bar{D} \to \gamma'\bar{\gamma}'} (T_{h}) Y_{D} (T_{h})^{2} + \langle \sigma v \rangle_{\gamma'\bar{\gamma}' \to D\bar{D}} (T_{h}) Y_{\gamma'} (T_{h})^{2} \right],$$

$$\frac{dY_{\gamma}'}{dT} = F(T) \left[\langle \sigma v \rangle_{D\bar{D} \to \gamma'\bar{\gamma}'} (T_{h}) Y_{D} (T_{h})^{2} - \langle \sigma v \rangle_{\gamma'\bar{\gamma}' \to D\bar{D}} (T_{h}) Y_{\gamma'} (T_{h})^{2} + \langle \sigma v \rangle_{i\bar{i} \to \gamma'} (T) Y_{i}^{eq} (T)^{2} - \left\langle \Gamma_{\gamma' \to i\bar{i}} (T_{h}) \right\rangle Y_{\gamma'} (T_{h}) \right],$$

$$F(T) \equiv -\frac{s}{H} \left(\frac{d\rho_{v}/dT}{4\zeta\rho - 4\zeta_{h}\rho_{h} + j_{h}/H} \right),$$
(5)

where s is the entropy density and v is the relative velocity. Dark photon is unstable and decays via the process $\gamma' \to 3\gamma$, and the entire relic density arises from the dark Dirac fermions D and \bar{D} so that

$$\Omega_D h^2 = s_0 m_D Y_D^0 h^2 / \rho_c, \tag{6}$$

where s_0 is the current entropy density, m_D is the mass of the D-fermion, Y_D^0 is Y_D at current times, and h is the Hubble parameter H_0 today in units of $100 \, \mathrm{km \, s^{-1} \, Mpc^{-1}}$. Using the above set of equations one can carry out a synchronous evolution of the visible and the hidden sectors and compute the ratio $\xi(T)$ (using the visible sector as a clock) by solving the coupled set of equations involving the $\xi(T)$ equation (3) and the yield equations (4) and (5).

We note that the yield equations involve two different temperatures on the right-hand side in equations (4) and (5). Thus, the objects

$$\langle \sigma v \rangle_{D\bar{D} \to \gamma' \gamma'} (T_h), \langle \sigma v \rangle_{\gamma' \gamma' \to D\bar{D}} (T_h), \langle \Gamma_{\gamma' \to i\bar{i}(T_h)} \rangle$$
 (7)

appearing on the right-hand side of equations (4) and (5) depend on the hidden sector temperature T_h while the quantities

$$\langle \sigma v \rangle_{i\bar{i} \to D\bar{D}}(T), \langle \sigma v \rangle_{i\bar{i} \to \gamma'}(T)$$
 (8)

depend on the visible sector temperature T indicating that a synchronous evolution of the thermal baths of the visible and the hidden sector is essential for a consistent solution to $\xi(T), Y_D(T_h), Y_{\gamma'}(T_h)$. However, here, the initial conditions at the reheat time on the hidden sector become relevant. Thus, as discussed earlier, the two extreme possibilities here are that at the reheat temperature the hidden sector either couples with the inflaton as strongly as the visible sector does where $\xi_0 \simeq 1$ and we have a hot hidden sector initially, or alternately, it does not couple with the inflaton at all or couples very feebly where $\xi_0 \sim 0$ and we have a cold hidden sector initially. We exhibit the effects of the initial conditions on the hidden sector in Figure 1. The analysis shows that the $\xi_0 = 1$ initial condition (hot hidden sector) gives a larger yield by O(100%) or more than the $\xi_0 = 0.01$ initial condition (cold hidden sector) highlighting the significant effect that the hidden initial condition has on the yield and on the relic density.

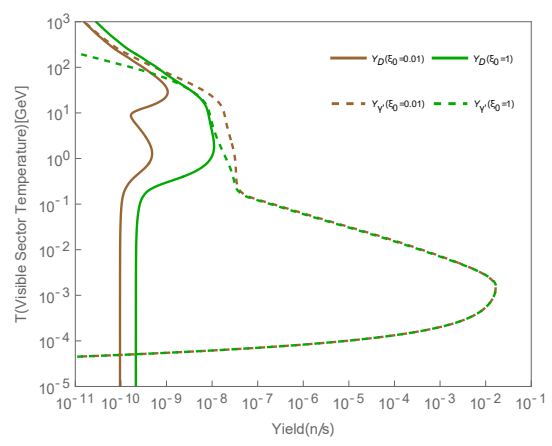


FIGURE 1: Yields of dark fermion (dark matter) and dark photon for a cold hidden sector at T_{RH} , i.e., $\xi_0 = 0.01$ (Brown) and a hot hidden sector at T_{RH} , i.e., $\xi_0 = 1$ (Green). The model parameters are $m_D = 2$ GeV, $m_{\gamma'} = 1.22$ MeV, $g_x = 0.019$, and $\delta = 4 \times 10^{-9}$. The relic density for $\xi_0 = 0.01$ is 0.0524 while that for $\xi_0 = 1$ is 0.117. The shift in the relic density from an initially hot hidden sector to an initially cold hidden sector is $\mathcal{O}(100\%)$.

3.2. Sommerfeld Enhancement of Dark Matter Cross Sections We discuss now the effects on Sommerfeld enhancement of dark matter cross sections when the hidden sector is hot vs cold at the reheat temperature in the early universe. The dark matter cross sections arise from various contributions, i.e., $DD \rightarrow DD$, $\bar{D}\bar{D} \rightarrow \bar{D}\bar{D}$, and $D\bar{D} \rightarrow D\bar{D}$. The interactions governing the scatterings arise from the exchange of dark photons, and in the nonrelativistic limit, the potential governing the scattering takes the form

$$V(r) = \pm \frac{(g_x)^2}{4\pi} \frac{e^{-m_{\gamma'}r}}{r}.$$
 (9)

Here, $DD \to DD$ and $\bar{D}\bar{D} \to \bar{D}\bar{D}$ scattering yield a (repulsive) Yukawa potential with a plus sign while the $D\bar{D} \to D\bar{D}$ scattering yields (an attractive) Yukawa potential with a negative sign. However, at low velocities, nonperturbative effects via exchange of multiple dark photons become significant and must be taken into account. These effects are typically summarized by the Sommerfeld enhancement factor S_E so that for the scattering process $A + B \to A + B$ one writes

$$(\sigma_{AB}v) = S_E \left(\sigma_{AB}^0 v\right),\tag{10}$$

where $(\sigma_{AB}^0 v)$ is the Born approximation and v is the relative velocity of the colliding particles. Such nonperturbative effects generated by the repeated exchange of a dark photon or from the exchange of some other mediators have been discussed by a number of previous authors (see, e.g., [18, 19, 20, 21, 22, 23] and the references therein).

To take into account the nonperturbative effects, we numerically solve the radial Schrödinger equation given by

$$p^{2}R_{l} + \frac{d^{2}R_{l}}{dr^{2}} + \frac{2}{r}\frac{dR_{l}}{dr} - \frac{l(l+1)R_{l}}{r^{2}} - 2\mu V(r)R_{l} = 0, \quad (11)$$

where p is the particle momentum, μ is the reduced mass, and V(r) is the Yukawa potential given by equation (9). Defining

x = pr and $R_{p,l} = Npu_l(x)/x$ leads to the following equation for $u_l(x)$ [24]:

$$\left(\frac{d^2}{dx^2} + 1 - \frac{l(l+1)}{x^2} - \frac{2ae^{-bx}}{x}\right) u_l(x) = 0,$$

$$a = \pm \frac{\mu g_X^2}{4\pi p}, \quad b = \frac{m_{\gamma'}}{p}.$$
(12)

The differential equation (12) has a solution of the following form:

$$\Phi_l(x)_{x\to\infty} \to C \sin\left(x - \frac{l\pi}{2} + \delta_l\right),$$
(13)

where δ_l is the lth partial wave phase shift. The Sommerfeld enhancement for the lth partial wave cross section for the case of the Yukawa potential is then given by

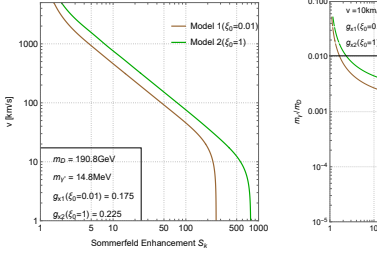
$$\sigma_l = S_{El} \cdot \sigma_{0,l},\tag{14}$$

where [24], $S_{El} = (1 \cdot 3 \cdots (2l+1)/C)^2$. Using equation (13), we get

$$C^{2} = \Phi_{l}^{2}(x)_{x \to \infty} + \Phi_{l}^{2} \left(x - \frac{\pi}{2} \right)_{x \to \infty},$$

$$S_{El} = \frac{((2l+1)!!)^{2}}{\Phi_{l}^{2}(x)_{x \to \infty} + \Phi_{l}^{2} \left(x - \frac{\pi}{2} \right)_{x \to \infty}}.$$
(15)

The analysis gives an enhancement of the dark matter cross section at low collision velocities for attractive potentials and a suppression for the case of repulsive potential. The analysis shows that the enhancement is very sensitive to ξ_0 . In Figure 2, we exhibit this sensitivity. Here, one finds that an initially hot hidden sector (i.e., $\xi_0=1$) gives a Sommerfeld enhancement which could be several orders of magnitude larger than the case for an initially cold hidden sector.



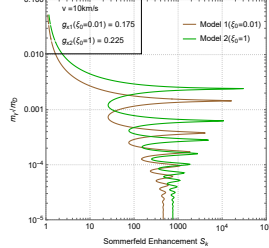


FIGURE 2: An exhibition of the effect of a hot vs a cold hidden sector at reheat on the *S*-wave Sommerfeld enhancement of dark matter cross section for an attractive Yukawa potential. The model parameters are $m_D = 190.8 \,\mathrm{GeV}$, $m_{\gamma'} = 14.8 \,\mathrm{MeV}$, and $\delta = 35.8 \times 10^{-9}$. Left panel: Sommerfeld enhancement factor at different relative velocities for a hot dark sector ($\xi_0 = 1$) and a cold dark sector ($\xi_0 = 0.01$). To keep the relic density ~ 0.12 , we choose $g_{x1} = 0.175$ for $\xi_0 = 0.01$ (Brown) and $g_{x2} = 0.225$ for $\xi_0 = 1$ (Green). Right panel: Sommerfeld enhancement factor vs $m_D/m_{\gamma'}$ with g_{x1} and g_{x2} from left panel.

3.3. N_{eff} at BBN for Hot vs Cold Hidden Sector

 $N_{\rm eff}$ represents the number of massless neutrino degrees of freedom beyond those of the standard model and is constrained by experimental data on the possible corridor between

experiment and the standard model prediction in which it can reside. It acts as a strong constraint on model building which involves new degrees of freedom that contribute to $\Delta N_{\rm eff}$. Thus, let us suppose that the hidden sector has $g_{\rm eff}^h(T_h)$ massless degrees of freedom at temperature T_h which is synchronous with temperature T in the visible sector. In this case, its contribution to $\Delta N_{\rm eff}$ is given by

$$\Delta N_{\text{eff}} = \frac{4}{7} g_{\text{eff}}^{h} (T_h) \left(\frac{11}{4}\right)^{4/3} \left(\frac{T_h}{T}\right)^{4}. \tag{16}$$

The standard model prediction for $N_{\rm eff}$ is 3.06 while the combined result from the Planck Collaboration [25] and the joint BBN analysis of deuterium/helium abundance gives $N_{\rm eff}^{\rm exp}=3.41\pm0.45$. A conservative constraint on the extra degrees of freedom is $\Delta N_{\rm eff}\leq 0.25$. We may contrast this with the dispersion in $\Delta N_{\rm eff}$ created by the choice of a hot initial hidden sector or a cold initial hidden sector as illustrated in Figure 3 for three value sets for the parameters $\{m_D,m_{\gamma'},g_x,\delta\}$. This figure illustrates a huge effect arising from the initial conditions for the hidden sector due to the factor $g_{\rm eff}^h(T_h)(T_h/T)^4$ which calls for an accurate computation of $\xi(T)$ for a reliable estimate of $\Delta N_{\rm eff}$ for a hidden sector model.

A comment is in order regarding equation (16) which requires that the hidden sector be in thermal equilibrium. This comes about as follows: while the hidden sector is not in thermal equilibrium with the visible sector because of feeble couplings between them, this does not apply to internal thermal equilibrium for the hidden sector. This is so because the couplings between the dark photons and the dark fermions and among other dark particles that may be around are not feeble but have normal strength and thermal equilibrium is established fairly quickly in thermal evolution. Further, $g_{\text{eff}}^h(T_h)$ is temperature dependent; thus, the temperature dependence for the hidden sector degrees is not exactly T_h^4 but governed the T_h dependence arising from the product $g_{\text{eff}}^{h}(T_h)T_h^4$. The exact computation of g_{eff}^h is done via thermal integrals and is exhibited in Appendix A. A further discussion of this topic can be found in [5, 6, 7, 17, 26].

3.4. On the Validity of Separate Entropy Conservation Approximation of Comoving Visible and Hidden Sector Volumes

In the thermal evolution of the visible and the hidden sector from early times, to later times a decoupling approximation is often used which assumes that the entropy densities of the visible and the hidden sectors are separately conserved in comoving volumes. This leads to the result that the ratio $s_h(T)/s_v(T)$ remains unchanged as the temperature evolves from the reheat temperature $T_0 = T_{RH}$ down to the temperature at BBN time and to the current temperature. This assumption gives the relation

$$\frac{h_{\text{eff}}^{h}(\xi(T)T)}{h_{\text{eff}}^{v}(T)}\xi^{3}(T) = \frac{h_{\text{eff}}^{h}(\xi(T_{0})T_{0})}{h_{\text{eff}}^{v}(T_{0})}\xi^{3}(T_{0}), \qquad (17)$$

where we used $T_h = \xi(T)T$ and $T_{0h} = \xi_0 T_0$. Equation (17) allows a computation of $\xi(T)$ using degrees of freedom at different temperatures. However, one may note that equation (17) has a highly nonlinear dependence on $\xi(T)$, and one needs a numerical integration using thermal integrals. Here, for the

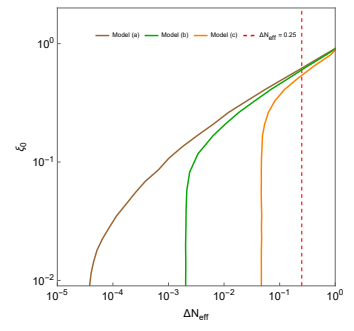


FIGURE 3: Exhibition of the dependence of $\Delta N_{\rm eff}$ at BBN time on ξ_0 in the range $\xi_0=(0,1)$. Models (a)–(c) are defined by the parameter set $\{m_D,m_{\gamma'},g_X,\delta\}$ with value sets: (a) $\{0.767\,{\rm GeV},0.406\,{\rm MeV},0.00984,2.88\times10^{-9}\}$; (b) $\{0.548\,{\rm GeV},0.618\,{\rm MeV},0.0121,87.0\times10^{-9}\}$; (c) $\{0.796\,{\rm GeV},0.960\,{\rm MeV},0.0159,654\times10^{-9}\}$. The analysis shows that $\Delta N_{\rm eff}$ at BBN can vary between $\Delta N_{\rm eff}=1$ for a hot hidden sector $(\xi_0=1)$ at the reheat and $\Delta N_{\rm eff}=10^{-5}$ for a cold hidden sector $(\xi_0=0)$ at the reheat due to the suppression factor $(T_h/T)^4$ pointing to the precision needed in the computation of $\xi(T_{\rm BBN})$. The dashed line indicates the approximate upper limit of the error corridor for new degrees of freedom in model building. The analysis is consistent with all known constraints on the hidden sector [27].

hidden sector, we will use the thermal integrals for the entropy degrees of freedom for γ' and D as given below [28, 29]:

$$h_{\text{eff}}^{\gamma'}(T_h) = \frac{45}{4\pi^4} \int_{x_{hn'}}^{\infty} \frac{\sqrt{x^2 - x_{h\gamma'}^2}}{e^x - 1} \left(4x^2 - x_{h\gamma'}^2\right) dx, \qquad (18)$$

$$h_{\text{eff}}^{D}(T_{h}) = \frac{15}{\pi^{4}} \int_{x_{hD}}^{\infty} \frac{\sqrt{x^{2} - x_{hD}^{2}}}{e^{x} + 1} \left(4x^{2} - x_{hD}^{2}\right) dx, \tag{19}$$

where $x_{h\gamma'} = m_{\gamma'}/(T_h) = m_{\gamma'}/(\xi(T)T)$ and $x_{hD} = m_D/(\xi(T)T)$. For the visible sector, thermal integrals of the above type are not known because of the hadronization of quarks and gluons and the degrees of freedom are given in terms of a table or a curve as a function of temperature [28, 29].

Figure 4 gives a comparison of the evolution of $\xi(T)$ as a function of the temperature *T* of the visible sector using the exact formula of equation (3) (solid lines) vs the one using the approximation of entropy conservation of the visible and the hidden sector separately in comoving volumes given by dashed lines. Thus, the left panel gives the analysis for different values of ξ_0 . Here, one finds significant deviations in the approximate results from the exact ones with the worst case occurring for the smallest ξ_0 case corresponding to the coldest hidden sector at the reheat temperature. The right panel gives the result for different values of the kinetic mixing parameter δ for a fixed value of ξ_0 . Here, one finds that even for very feeble couplings with δ as small as $\delta = 10^{-12}$, there are significant deviations of the predictions on $\xi(T)$ at BBN time between the exact and the approximate. Thus, our conclusion is that entropy conservation approximation separately for comoving sectors of the visible and hidden sectors in thermal evolution is not suitable in general for precision cosmology.

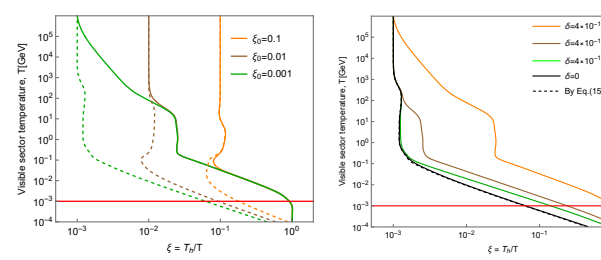


FIGURE 4: Evolution of $\xi(T)$ with different initial conditions using equation (3) of this paper (solid) and using the approximation of entropy conservation (dashed). Left panel: Here, $\delta=4\times10^{-10}$ and analysis is given for three widely different values of ξ_0 , i.e., $\xi_0=0.001$, $\xi_0=0.01$, $\xi_0=0.1$. Right panel: Here, $\xi_0=0.001$ and an analysis of several different values for δ in the range from $\delta=0$ to $\delta=10^{-10}$ is exhibited. The rest of the parameters are chosen so that $m_D=2$ GeV, $m_{\gamma'}=1.22$ MeV, and $g_X=0.019$.

4. CONCLUSION

The analysis discussed here exhibits the fact that the thermal condition of the hidden sector at reheat temperature affects observables related to thermal relics. Thus, assumptions of a hot vs a cold hidden sector at reheat can lead up to O(100%) shift on predicted values of observables and for $\Delta N_{\rm eff}$ by as much as a factor of 10^5 due to the large variation generated by the factor $(\frac{T_h}{T})^4$ as T_h/T varies. It is also shown that the approximation of using entropy conservation in comoving volumes for the visible and the hidden sectors is invalid even for very feeble couplings between the visible and the hidden sectors.

Appendix A. ENERGY DENSITY OF HIDDEN SECTOR

Assuming for illustration just dark photon (γ') and dark fermion (D) in the hidden sector, the energy density of the hidden sector $\rho_h(T_h)$ is given by

$$\rho_{h}(T_{h}) = \rho_{\gamma'}(T_{h}) + \rho_{D}(T_{h}) = \frac{\pi^{2}}{30}g_{\text{eff}}^{h}(T_{h})T_{h}^{4},$$

$$\rho_{\gamma'}(T_{h}) = \frac{\pi^{2}}{30}g_{\text{eff}}^{\gamma'}(T_{h})T_{h}^{4},$$

$$\rho_{D}(T_{h}) = \frac{\pi^{2}}{30}g_{\text{eff}}^{D}(T_{h})T_{h}^{4},$$

$$g_{\text{eff}}^{h}(T_{h}) = g_{\text{eff}}^{\gamma'}(T_{h}) + g_{\text{eff}}^{D}(T_{h})$$

$$= \frac{45}{\pi^{4}}\int_{x_{\gamma}^{\prime}}^{\infty} \frac{\sqrt{x^{2} - x_{\gamma'}^{2}}}{e^{x} - 1}x^{2}dx + \frac{60}{\pi^{4}}\int_{x_{D}}^{\infty} \frac{\sqrt{x^{2} - x_{D}^{2}}}{e^{x} + 1}x^{2}dx,$$
(A.2)

where $x_{\gamma'} = m_{\gamma'}/T_h$, and $x_D = m_D/T_h$. Thus, $g_{\rm eff}^h(T_h)$ is temperature dependent and the effective temperature that enters in equation (16) is not just T_h^4 but $g_{\rm eff}^h(T_h)T_h^4$.

CONFLICTS OF INTEREST

The authors declare that there are no conflicts of interest regarding the publication of this paper.

ACKNOWLEDGMENTS

This research was supported in part by the NSF Grant PHY-2209903.

References

- P. Nath, Cambridge University Press, 2016,
 ISBN 978-0-521-19702-1, 978-1-316-98396-6
 doi:10.1017/9781139048118
- [2] P. Candelas, G. T. Horowitz, A. Strominger, and E. Witten, Nucl. Phys. B 258, 46–74 (1985) doi:10.1016/0550-3213(85)90602-9
- [3] J. Polchinski, [arXiv:hep-th/9611050 [hep-th]].
- [4] C. T. Hill, S. Pokorski, and J. Wang, Phys. Rev. D 64, 105005 (2001) doi:10.1103/PhysRevD.64.105005
 [arXiv:hep-th/0104035 [hep-th]].
- [5] A. Aboubrahim, W. Z. Feng, P. Nath, and Z. Y. Wang, Phys. Rev. D 103, no.7, 075014 (2021) doi:10.1103/PhysRevD.103.075014 [arXiv:2008.00529 [hep-ph]].
- [6] A. Aboubrahim, W. Z. Feng, P. Nath, and Z. Y. Wang, JHEP 06, 086 (2021) doi:10.1007/JHEP06(2021)086 [arXiv:2103.15769 [hep-ph]].
- [7] A. Aboubrahim and P. Nath, JHEP 09, 084 (2022) doi:10.1007/JHEP09(2022)084 [arXiv:2205.07316 [hep-ph]].
- [8] J. L. Feng, H. Tu, and H. B. Yu, JCAP 10, 043 (2008) doi:10.1088/1475-7516/2008/10/043 [arXiv:0808.2318 [hep-ph]].
- [9] F. Ertas, F. Kahlhoefer, and C. Tasillo, JCAP 02, no.02, 014 (2022) doi:10.1088/1475-7516/2022/02/014 [arXiv:2109.06208 [astro-ph.CO]].
- [10] B. Holdom, Phys. Lett. B **166**, 196–198 (1986) doi:10.1016/0370-2693(86)91377-8
- [11] B. Kors and P. Nath, Phys. Lett. B **586**, 366–372 (2004) doi:10.1016/j.physletb.2004.02.051 [arXiv:hep-ph/0402047 [hep-ph]].
- [12] D. Feldman, Z. Liu, and P. Nath, Phys. Rev. D 75, 115001 (2007) doi:10.1103/PhysRevD.75.115001 [arXiv:hep-ph/0702123 [hep-ph]].
- [13] M. Du, Z. Liu, and P. Nath, Phys. Lett. B 834, 137454 (2022) doi:10.1016/j.physletb.2022.137454 [arXiv:2204.09024 [hep-ph]].
- [14] B. Patt and F. Wilczek, [arXiv:hep-ph/0605188 [hep-ph]].
- [15] K. Cheung and T. C. Yuan, JHEP **03**, 120 (2007) doi:10.1088/1126-6708/2007/03/120 [arXiv:hep-ph/0701107 [hep-ph]].
- [16] A. Aboubrahim, P. Nath, and Z. Y. Wang, JHEP 12, 148 (2021) doi:10.1007/JHEP12(2021)148 [arXiv:2108.05819 [hep-ph]].
- [17] J. Li and P. Nath, Phys. Rev. D 108, no.11, 115008 (2023) doi:10.1103/PhysRevD.108.115008 [arXiv:2304.08454 [hep-ph]].
- [18] M. Lattanzi and J. I. Silk, Phys. Rev. D 79, 083523 (2009) doi:10.1103/PhysRevD.79.083523 [arXiv:0812.0360 [astro-ph]].
- [19] N. Arkani-Hamed, D. P. Finkbeiner, T. R. Slatyer, and N. Weiner, Phys. Rev. D 79, 015014 (2009) doi:10.1103/PhysRevD.79.015014 [arXiv:0810.0713 [hepph]].

- [20] S. Cassel, J. Phys. G 37, 105009 (2010) doi:10.1088/0954-3899/37/10/105009 [arXiv:0903.5307 [hep-ph]].
- [21] M. Cirelli, A. Strumia, and M. Tamburini, Nucl. Phys. B **787**, 152–175 (2007) doi:10.1016/j.nuclphysb.2007.07.023 [arXiv:0706.4071 [hep-ph]].
- [22] T. Bringmann, F. Kahlhoefer, K. Schmidt-Hoberg, and P. Walia, Phys. Rev. Lett. 118, no.14, 141802 (2017) doi:10.1103/PhysRevLett.118.141802 [arXiv:1612.00845 [hep-ph]].
- [23] J. L. Feng, M. Kaplinghat, H. Tu, and H. B. Yu, JCAP 07, 004 (2009) doi:10.1088/1475-7516/2009/07/004 [arXiv:0905.3039 [hep-ph]].
- [24] R. Iengo, JHEP **05**, 024 (2009) doi:10.1088/1126-6708/2009/05/024 [arXiv:0902.0688 [hep-ph]].
- [25] N. Aghanim et al. [Planck], Astron. Astrophys. 641, A6 (2020) [erratum: Astron. Astrophys. 652, C4 (2021)] doi:10.1051/0004-6361/201833910 [arXiv:1807.06209 [astro-ph.CO]].
- [26] A. Aboubrahim, M. Klasen, and P. Nath, JCAP **04**, no.04, 042 (2022) doi:10.1088/1475-7516/2022/04/042 [arXiv:2202.04453 [astro-ph.CO]].
- [27] A. Aboubrahim, M. M. Altakach, M. Klasen, P. Nath, and Z. Y. Wang, JHEP 03, 182 (2023) doi:10.1007/JHEP03(2023)182.01268 [hep-ph]].
- [28] M. Hindmarsh and O. Philipsen, Phys. Rev. D 71, 087302
 (2005) doi:10.1103/PhysRevD.71.087302 [arXiv:hep-ph/0501232 [hep-ph]].
- [29] L. Husdal, Galaxies 4, no.4, 78 (2016) doi:10.3390/galaxies4040078 [arXiv:1609.04979 [astro-ph.CO]].